Metallic Fuels

Microstructural and Diffraction Studies on Th-U and Th-U-Mo Alloys

Raj Kumar[1]*, Sourabh Wajhal[2], Sonal Gupta[1], A.B. Shinde[2], PSR Krishna[2], S.K. Satpati[1], M.L. Sahu[1]

[1]*Uranium Extraction Division, Bhabha Atomic Research Centre, Mumbai-400085, INDIA*
[2]*Solid State Physics Division, Bhabha Atomic Research Centre, Mumbai-400085, INDIA*

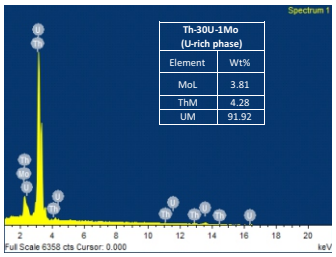

EDS of the alloys

ABSTRACT

The motivation behind the present study is the resurgence of interest in the metallic fuels and attractive nuclear properties of thorium metal/alloys. In the present study, microstructural and diffraction studies on Th-U-Mo alloys have been presented. Molybdenum was added to the alloys to stabilize uranium as isotropic γ-U phase, to increase fissile loading beyond 20wt% uranium. The microstructures of the alloys were studied using optical microscopy and SEM, and composition of the various phases was determined using EDS. The structural studies were carried out using X-ray and neutron diffraction, and the quantitative estimation of γ-U phase in Th-U-Mo alloys was done using Rietveld method on polycrystalline samples.

KEYWORDS: Metallic fuel, Thorium, Microstructure, X-ray diffraction, Neutron diffraction, Fissile loading, Gamma-Uranium phase

Introduction

Metallic fuels based on uranium were used in the early days of the nuclear energy programme, back in 1960s [1-3]. However, the focus gradually shifted towards ceramic fuels, mainly oxide (UO_2) owing to its higher melting point, fission product accommodation due to relatively open structure and thus higher burnup [2-5]. Recently, there has been resurgence in interest towards metallic fuels, since mid-1980s, owing to their numerous advantages e.g. higher fissile content, better thermal conductivity, ease of fabrication, higher breeding ratio, better inherent safety performance owing to its reduced Doppler reactivity mechanism[2-3, 6-8].

However, uranium based metallic fuels pose certain concerns for fuel designers, viz., irradiation growth, swelling, anisotropic crystal structure of the candidate fuel etc. [2-3, 9]. Metallic fuels based on thorium appear to be better in several aspects than the uranium based metallic fuels. Thorium has isotropic crystal structure, higher melting point, higher thermal conductivity and negligible fission gas swelling [2-3, 10-11]. However, the deployment of thorium based metallic fuels will need sufficient data in terms of their microstructure and phase stability, thermal properties, irradiation stability etc.

Preliminary work on Th-U alloys has been done in late 50s and early 60s.However, favorable properties of thorium based metallic fuels in terms of higher fissile content, higher thermal conductivity, higher breeding gain etc. compared to oxide fuels have gathered renewed research interest in it [2-3, 11-12].

Sustainability of the nuclear energy in the long term will need harnessing of more abundant fertile materials viz. ^{238}U and ^{232}Th in addition to the use of fissile ^{235}U [2, 11, 13-14]. Utilisation of thorium in Indian Nuclear Energy Programme was envisaged in the very beginning itself. Thorium is 3-4 times more abundant than uranium[13-14]. In the context of Indian scenario, where thorium reserves are vast as compared to leaner reserves of uranium, makes it a strong case for development of thorium-based fuels and reactors. Thorium exists as ^{232}Th which is not fissile like ^{235}U, ^{239}Pu or ^{233}U, the fertile thorium needs to be converted into fissile ^{233}U before it can be used as a nuclear fuel. Thorium being fertile, needs to be combined with fissile material for conversion to fissile ^{233}U. ^{232}Th-^{233}U fuel cycle can be used in thermal as well as in fast neutron spectrum in contrast to ^{238}U-^{239}Pu fuel cycle which can be used only in the fast neutron spectrum [13, 15].

Uranium rich phase is finely dispersed in the f.c.c. thorium matrix in Th-(<20wt%)U alloys. With increase beyond 20wt%, uranium forms continuous metallic network at the grain boundaries and eventually becomes the continuous phase[12, 14, 16-18]. Microstructure of this kind is not favourable from radiation stability aspect as undesirable characteristics of α-U e.g. an isotropy, dimensional instability, swelling, thermal cycling growth etc. start dominating[17]. Fine uranium dispersion in the microstructure helps in (a) depositing the fission fragments outside uranium matrix directly in the thorium matrix, (b) anchoring gas filled pores and (c) lowering gas diffusion rates due to high melting point of thorium[17-18]. Excellent radiation stability was observed in Th-(<20wt%)U alloys in irradiation studies, corroborating the above fact [19]. To increase fissile loading beyond 20wt% in Th-U alloys, uranium should be stabilised as isotropic γ-U phase. Hence, uranium needs to be alloyed with gamma stabilizers e.g. Mo, Zr, Nb etc. Farkas et al. have reported few preliminary studies on the ternary additions of Mo, Nb and Zr in Th-U binary alloys. Molybdenum is one of the best stabilisers of γ-U at room temperature[20-22]. The aim of these studies is to improve the irradiation resistance by stabilizing the γ-U phase as well as enhancing the high temperature strength of the alloy [17].

*Author for Correspondence: Raj Kumar
E-mail: rajk@barc.gov.in

In the present work, microstructural and diffraction studies on the Th-U-Mo alloys have been carried out. The structural studies were carried out using X-ray and neutron diffraction, and the quantitative estimation of γ-U phase in Th-U-Mo alloys was done using Rietveld method on polycrystalline samples.

Experimental Details

The starting materials for the preparation of Th-U and Th-U-Mo alloys were thorium finger, uranium and molybdenum slugs. Thorium finger was prepared by consolidating thorium powder which was obtained by calciothermic reduction of thoria followed by leaching. Molybdenum was obtained from M/s Midhani, Hyderabad, India. Uranium slugs of nuclear purity were obtained from AFD, BARC. Details of the starting material are given in Table 1.

Table 1: Details of the starting materials.

Material	Assay (wt%)	Oxygen (wt%)	Nitrogen (wt%)	Carbon (wt%)
Thorium powder	99.5	0.117 ± 0.012	0.0050 ± 0.0005	0.016 ± 0.001
Uranium	99.9	-	0.0140 ± 0.0010	0.010 ± 0.001
Molybdenum slugs	>99.9	-	-	-

Alloys were prepared by melting the constituents in water cooled copper hearth in a non-consumable arc melting set-up. The chamber was evacuated three times and back filled with high purity argon, before proceeding for melting of the alloys. Further, zirconium sponge was melted first, to consume residual oxygen and nitrogen present in the melting chamber. Alloys were then re-melted five times in arc melting setup under inert atmosphere each time turning the alloy piece upside down to ensure homogeneity of the constituents in the alloys. Molten alloys were suction cast in to 5 mm diameter cylindrical rods.

Carbon, oxygen and nitrogen content were also determined in addition to the assay content of the metals and alloys. The principle of inert gas fusion and thermal conductivity detection was used for the determination of nitrogen. The principle of combustion of sample followed by infrared (IR) detection was used for determination carbon. Oxygen was determined based on the principles of inert gas fusion and infrared (IR) detection.

Optical microstructures of the alloys were observed in an inverted optical microscope (M/s Olympus, Japan; Model: GX-51). Halogen light source (100W) was used in combination with light filters according to the requirement. Micrographs were captured using digital camera (M/s Olympus; Color View 1) attached to it. Optical images were obtained in bright field mode. Controlled oxidation of the alloys gave the best contrast in the optical microscopy.

Alloy samples were encapsulated in quartz tubes under vacuum of 10^{-3} mbar and then homogenized at 1000 °C (γ-U phase region) for 24 hours. One set of alloys was water quenched (WQ) and one set of alloys was allowed to cool inside the furnace itself, i.e., slow cooling (SC). Th-30U-2Mo and Th-30U-3Mo were subsequently aged at 500 °C below the eutectoid decomposition temperature of γ-U (580 °C).

Phase characterizations were done using an XRD unit with curved position sensitive detector (M/s INEL, France, Model: Equinox 3000) at 40kV and 30mA with Cu K_α(1.54056 Å) radiation. The diffractometer is calibrated using standard yttria sample.

Scanning electron microscope (SEM) having secondary electron detector (SE, Everhart Thornley) and back scattered electron detector (BSE) was used for electron microscopy. The energy dispersive spectroscopy with Si(Li) detector was employed for qualitative elemental mapping.

Neutron diffraction experiment was performed at Powder Diffractometer 2 (PD-2) at Dhruva research reactor, BARC. The wavelength of monochromatic neutrons was 1.2443 Å. Data collections were performed in Debye-Scherrer geometry in the 2θ range 6°-135° with a step size of 0.1°. The air background was subtracted from the collected data prior to analysis. The alloy samples were in rod/plate form and the samples were mounted on a rotating stage to avoid the preferred orientation effects in the diffraction pattern. As neutrons can penetrate deep in the sample so the bulk samples can be studied which is advantageous in obtaining correct quantitative phase analysis.

Results and Discussion

Chemical Analysis of Thorium Metal and Alloy

Chemical analyses of the starting thorium metal and alloy used in the present study and that used by previous investigators are presented in Table 2. Both thorium and uranium have got strong affinity for carbon, nitrogen and

Table 2: Chemical Analysis Results of Thorium Metal & Alloy used in the Present Work and by Previous Investigators.

Sample \ Element (wt%)		Th	U	Mo	O	C	N
Present Study	Th metal finger	99.5 ± 0.1	-	-	0.139 ± 0.014	0.041 ± 0.004	0.03 ± 0.003
	Th-30U-3Mo	64.1 ± 0.1	33.2 ± 0.1	2.7 ± 0.1	0.179 ± 0.018	0.047 ± 0.004	0.045 ± 0.004
Previous reported work	Th metal and alloys	Bentle[23](1958)			0.131	0.040	0.008
					0.029	0.005	0.001
		Bannister et al.[24] (1964)			0.2 - 0.3	0.001 - 0.015	-
		Hayward et al.[25] (1958)			0.1379	0.06 - 0.07	-

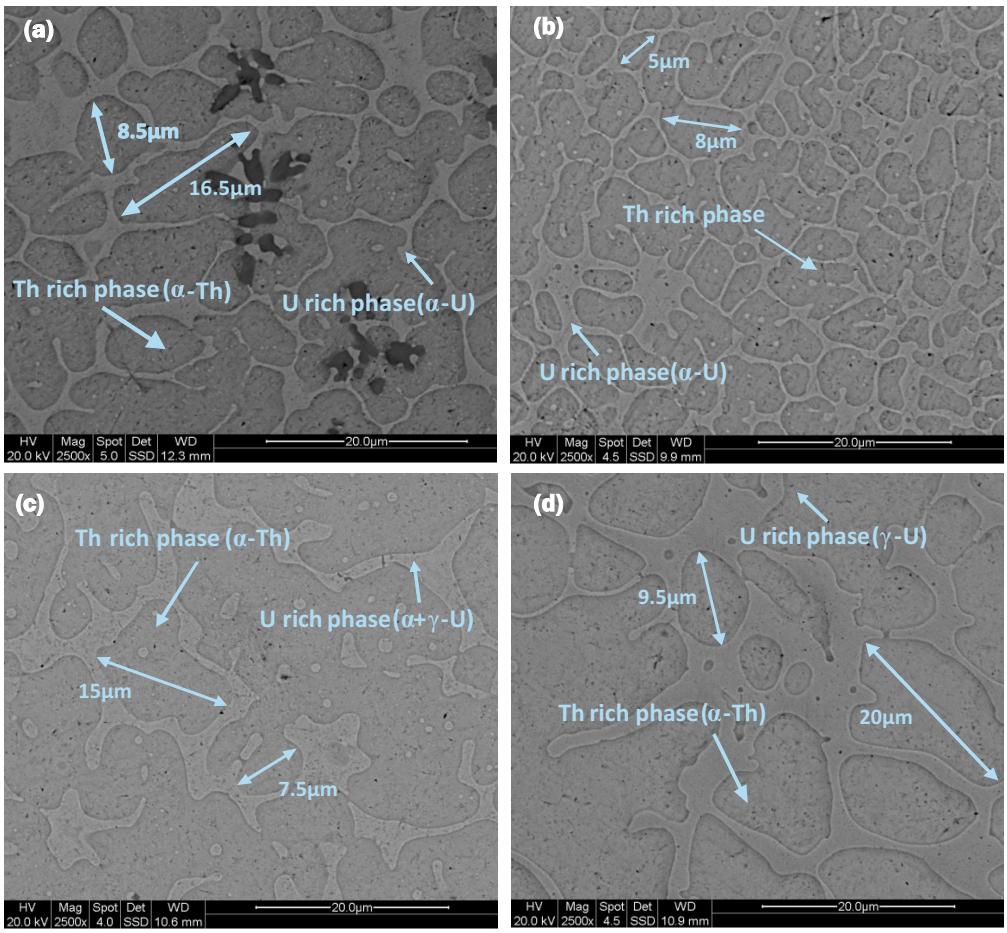

Fig.1: SEM Micrographs of the as-cast (a) Th-30U (b) Th-30U-1Mo (c) Th-30U-2Mo (d) Th-30U-3Mo.

oxygen. However, impurity content of this order does not have significant effect on the properties of thorium alloys. Carbon can significantly affect the mechanical properties of Thorium. Oxide inclusions as high as 3wt% do not seriously impair the mechanical fabrication. Homogeneity of the Th-U alloys depends on obtaining a reasonably fast cooling rate. Gravity segregation as well as carbon contamination from the graphite crucible are the major problems encountered in the induction melting of thorium. So, arc melting is better as it will offer faster cooling rate as well as the water-cooled copper crucible will avoid carbon contamination. The impurity content in the metal and alloys used in this study are comparable with that used by previous investigators.

Microstructures of the Alloys

The as–cast optical microstructures of the alloys are shown in Fig.1. The alloy microstructure is biphasic consisting of thorium rich and uranium rich phases. Interconnected network of uranium rich phase is present in a matrix of thorium rich phase. Uranium rich phase being the last to solidify, eventually solidifies in the grain boundary regions of the thorium rich phase and forms this kind of interconnected network upon solidification. The distribution of uranium in thorium matrix governs the irradiation behavior of Th-U alloys. Fine dispersion of uranium particles in the thorium matrix imparts dimensional stability and is favourable from fission gas retention point of view. Most of the fission fragments are deposited outside the uranium precipitate in the Th matrix and the fine dispersion of uranium particles helps to anchor the gas filled pores [13]. From the SEM images in Fig.1, it is quite evident that with addition of 1wt%Mo in the Th-30U alloy the grain structure becomes finer. With 2wt% Mo, however, the grain size increases and with further addition of 3wt% Mo the grain size increases further. As the grain boundaries could not be revealed in all the grains, conventional grain size measurement techniques could not be employed to measure the grain size.

Composition of the Various Phases

The SEM-EDS analysis of the Th-U-Mo alloys is shown in Fig.2. The U-rich phase and Th-rich phase were identified. Mo has formed solid solution with uranium and Mo was not detected in the Th rich phase in all the alloys as seen in the EDS results. Molybdenum has got appreciable solid solubility in uranium but has negligible solid solubility in thorium [26-27]. In this case, molybdenum has distributed itself according to its solubility in the uranium rich phase and thorium rich phase. EDS results are in good agreement with the target composition. The overall alloy composition of the alloys has also been confirmed by XRF.

Heat Treatment of the Alloys

Heat treatment of the alloys was done to evaluate the stability of the microstructure and the various phases. Homogenization of the alloys was done at 1000 °C for 24 hours to ensure homogeneous distribution of molybdenum and to rule out any instability of the γ-U phase due to inhomogeneous distribution of molybdenum. One set of alloy was allowed to be cooled in the furnace itself i.e. slow cooling (SC) and the other set of alloy was water quenched (WQ) i.e. fast cooling. Stabilization of γ-U phase in U-Mo alloys depends on the molybdenum content and the rate of cooling [28]. Microstructures of these alloys after homogenization treatment are shown in Fig.3. Networks of interconnected uranium formed at grain boundaries, became discrete in both

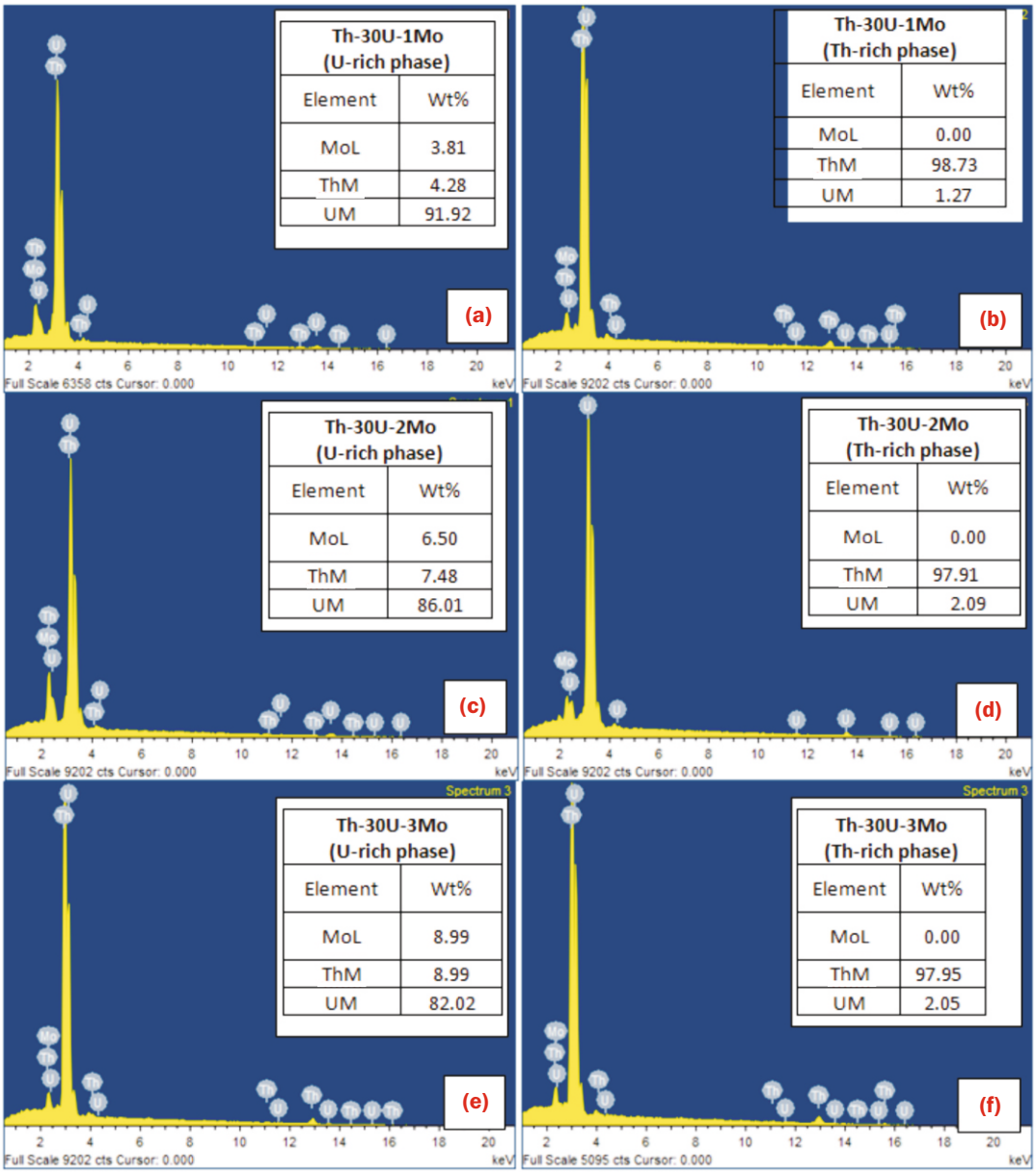

Fig.2: EDS of the alloys.

slow cooled as well as in water quenched condition. Dispersion of uranium in the form of globules from the interconnected network could be due to (i) minimization of surface energy and (ii) significant variation in the solid solubility of uranium in thorium with temperature. Studies by Bentleon the solid solubility of uranium in thorium from lattice parameter measurement has shown that solubility of uranium in thorium is less than 1 weight per cent at room temperature and increases to about 7 weight per cent at 1270°C [26]. The increase in solubility of uranium at higher temperature possibly causes some amount of uranium to get dissolved in the thorium rich phase. This causes breaking of the interconnected network of uranium rich phase. While cooling, due to decease in solubility, uranium reappears. Since everything is in solid state, smaller separated uranium globules are not able to coalesce with other particles and reappear as discrete globules. With faster cooling rate the globules are expected to be finer due to larger number of nucleation sites. Uranium dispersion was found to be finer under water quenched condition than that of slow cooled condition in the case of Th-30U-1Mo and Th-30U-2Mo alloys. However in case of Th-30U-3Mo, no major change in the microstructural features was observed, which needs further investigation.

Diffraction Studies

Room temperature x-rayand neutron diffraction patterns as shown in Fig.4 and Fig.5 confirms that γ-U phase is stabilized in Th-30U-2Mo and Th-30U-3Mo alloys. Th-30U and Th-30U-1Mo contained α-Th and α-U phases.

With higher molybdenum content the stability of the γ-U increases, which has been reported by several workers in binary U-Mo alloys [28-30]. The Th-30U-2Mo ternary alloy corresponds to a binary composition of U-6.25Mo.

With the addition of Mo in the system, the α-U changes to γ-U phase which exists in b.c.c. crystal structure and shows isotropic thermal expansion behaviour. With temperature the changes in the lattice are equal in all three directions and this is a desirable property to make nuclear fuel more stable. X-ray and neutron diffraction experiments were performed to quantify the phase fraction of γ-U with respect to Mo concentration.

a) Th-30U-3Mo: Neutron Diffraction

For Th-30U-3Mo system, most of the U was observed to be present in gamma phase. With incorporation of 3% Mo, complete γ-U phase stabilization was achieved.

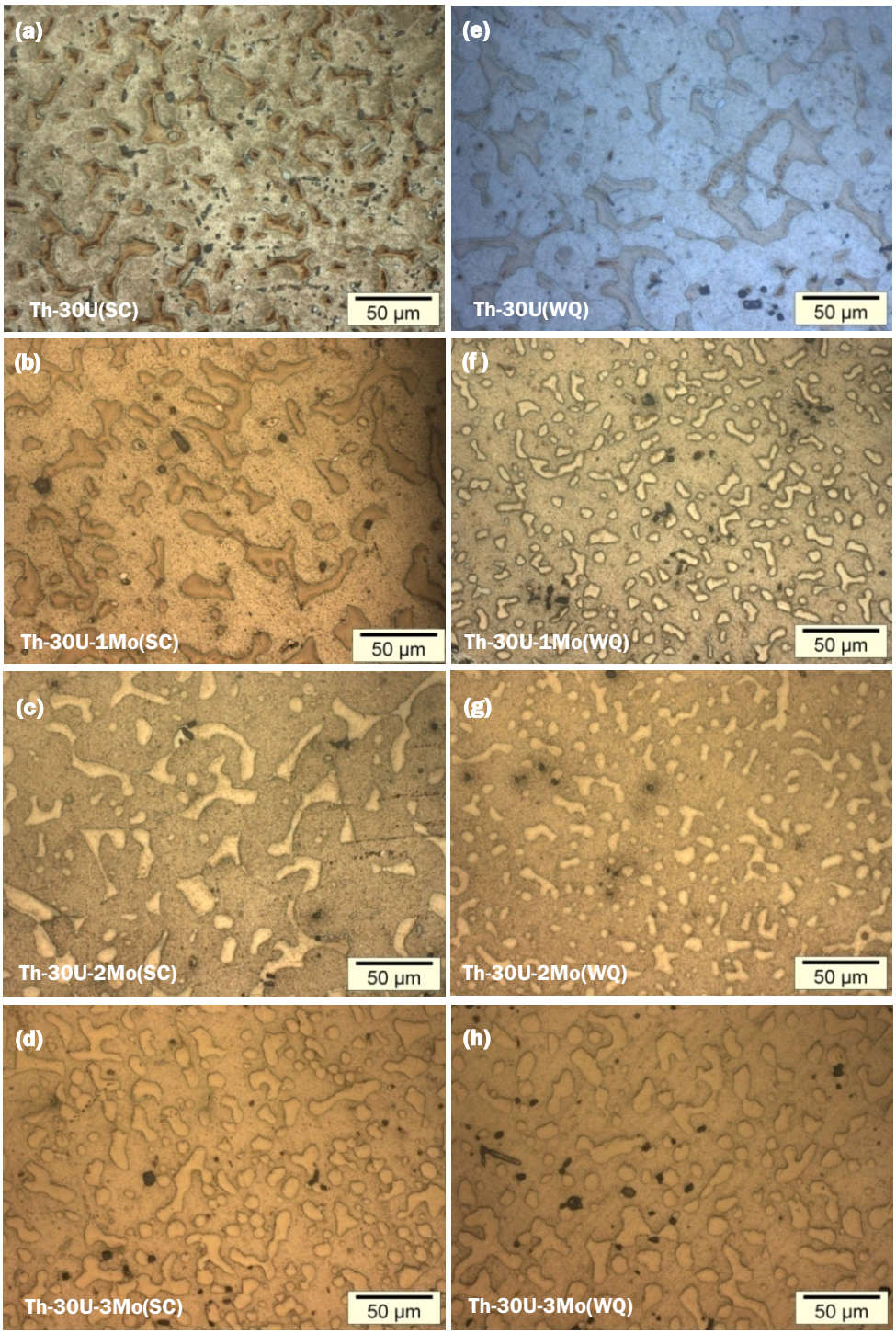

Fig.3: Optical Micrograph of Alloys Homogenised at 1000°C for 24 hours and slow cooled, SC (a-d) (a)Th-30U (b)Th-30U-1Mo (c)Th-30U-2Mo and (d) Th-30U-3Mo and water quenched, WQ (e-h)(e)Th-30U (f)Th-30U-1Mo (g)Th-30U-2Mo and (h) Th-30U-3Mo.

Weighted Average Bragg R-factor: 7.56

Rp: 4.46; Rwp: 5.63; Rexp: 3.39; Reduced Chi2: 2.75

b) Th-30U-3Mo: X-ray Diffraction

Weighted Average Bragg R-factor: 5.34

Rp: 11.5; Rwp: 14.7; Rexp: 9.55;

Reduced Chi2: 2.36

Table 3: Phase Fraction and Lattice Parameter data for Th-30U-3Mo (Neutron Diffraction) obtained by Rietveld method.

Phase	Space group	Phase fraction (%)	a (Å)	b (Å)	c (Å)	Angles
Th	F m - 3 m	68.28 ± 0.54	5.089(6)	5.089(6)	5.089(6)	α = 90°; ß = 90°; γ = 90°
U	I m - 3 m	28.56 ± 0.13	3.418(9)	3.418(9)	3.418(9)	α = 90°; ß = 90°; γ = 90°
ThO_2	F m - 3 m	3.16 ± 0.01	5.600(7)	5.600(7)	5.600(7)	α = 90°; ß = 90°; γ = 90°

For Th-30U-3Mo system, different values of ThO_2 crystalline phase fraction was observed in X ray and neutron diffraction studies. As the oxidation of Th is more prominent on surface and Cu K-α X rays probe the high Z materials on the surface, so a larger fraction (15%) of ThO_2 phase was detected through XRD.

Whereas neutrons with comparatively larger penetration depth will give us the more accurate information of the bulk. From neutron diffraction the ThO_2 phase fraction was estimated to be around 3% and this is in agreement with chemical analytical techniques. The authors propose that for such materials, neutron diffraction can be utilized which is non-destructive in nature. The Rietveld refinement fits for X-ray and neutron diffraction data of Th-30U-3Mo are presented in Fig. 4.

c) Th-30U: X-ray Diffraction

Weighted Average Bragg R-factor: 12.39

Rp: 12.1; Rwp: 15.5; Rexp: 9.09; Reduced Chi2: 2.90

d) Th-30U-2Mo: X-ray Diffraction

Weighted Average Bragg R-factor: 11.54

Rp: 11.2; Rwp: 14.5; Rexp: 8.84; Reduced Chi2: 2.69

e) Th-30U-1Mo: X-ray Diffraction

Weighted Average Bragg R-factor: 7.38

Rp: 9.80; Rwp: 12.6; Rexp: 8.91; Reduced Chi2: 1.98

The Rietveld refinement fits for X-ray diffraction data of the four alloy samples is presented in Fig. 5. In Th-U-Mo alloys, γ-U phase fraction in Th-U-Mo alloys is found to increase with increase in the concentration of molybdenum, which is depicted in Fig. 6.

Summary and Conclusion

1. The microstructures of the binary Th-30U as well as the ternary Th-30U-Mo alloys show interconnected networks of U rich phase at the grain boundaries. With 1wt% Mo addition in the Th-30U alloy the grain structure becomes finer. However, with addition of 2wt% and 3wt% Mo progressive increase in grain size was observed.

2. From the SEM-EDS analysis it was seen that all the molybdenum has formed solid solution with the

Table 4: Phase fraction and lattice parameter data for Th-30U-3Mo (X-ray diffraction) obtained by Rietveld method.

Phase	Space group	Phase fraction (%)	a (Å)	b (Å)	c (Å)	Angles
Th	F m - 3 m	56.13 ± 1.74	5.066(9)	5.066(9)	5.066(9)	α = 90°; ß = 90°; γ = 90°
γ - U	I m - 3 m	28.30 ± 1.19	3.425(6)	3.425(6)	3.425(6)	α = 90°; ß = 90°; γ = 90°
ThO_2	F m - 3 m	15.12 ± 1.46	5.577(13)	5.577(13)	5.577(13)	α = 90°; ß = 90°; γ = 90°

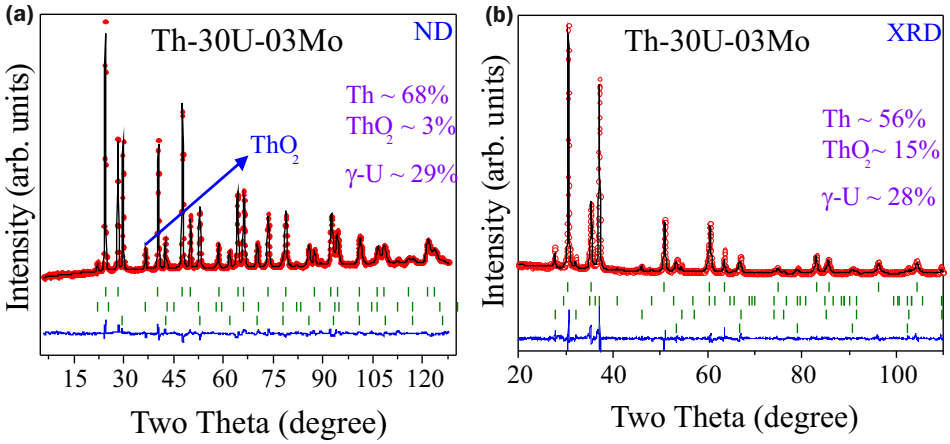

Fig.4: Rietveld refinement fit of Th-30U-3Mo sample : (a) Neutron Diffraction (b) X-ray Diffraction.

Table 5: Phase fraction and lattice parameter data for Th-30U (X-ray diffraction) obtained by Rietveld method.

Phase	Space group	Phase fraction (%)	a (Å)	b (Å)	c (Å)	Angles
Th	F m - 3 m	74.69 ± 3.01	5.086(14)	5.086(14)	5.086(14)	α = 90°; ß = 90°; γ = 90°
α - U	C m c m	23.73 ± 1.03	2.851(12)	5.875(12)	4.949(7)	α = 90°; ß = 90°; γ = 90°
ThO_2	F m - 3 m	1.58 ± 0.35	5.592(8)	5.592(8)	5.592(8)	α = 90°; ß = 90°; γ = 90°

Table 6 : Phase fraction and lattice parameter data for Th-30U-2Mo (X-ray diffraction) obtained by Rietveld method.

Phase	Space group	Phase fraction (%)	a (Å)	b (Å)	c (Å)	Angles
Th	F m - 3 m	76.78 ± 2.38	5.085(5)	5.085(5)	5.085(5)	α = 90°; ß = 90°; γ = 90°
α - U	C m c m	11.90 ± 2.20	2.839(6)	6.054(8)	4.842(10)	α = 90°; ß = 90°; γ = 90°
ThO_2	F m - 3 m	1.25 ± 0.29	5.576(7)	5.576(7)	5.576(7)	α = 90°; ß = 90°; γ = 90°
γ - U	I m - 3 m	10.08 ± 0.70	3.419(4)	3.419(4)	3.419(4)	α = 90°; ß = 90°; γ = 90°

uranium and negligible Mo was detected in the Th rich phase. The Mo concentration obtained as per the EDS results is in good agreement with the target alloy compositions.

3. It was observed that after the homogenization treatment at 1000°C for 24 hours, the interconnected networks of the uranium formed at grain boundaries become discrete, which is favourable from irradiation stability point of view.

4. The microstructure and phase composition of Th-30U-3Mo alloy were observed to be quite stable after ageing at 500°C for up to one month.

5. From the diffraction studies and Rietveld refinement, it is concluded that in Th-30U-2Mo, γ-U phase has been partially stabilized and in Th-30U-3Mo, it has been fully stabilized at room temperature. It has also been observed that for the quantification of thorium oxide phase, neutron diffraction is better than x-ray diffraction.

6. Th-30U-3Mo in as cast condition consists of uranium in isotropic gamma phase and is likely to be better than the corresponding binary Th-U as well as the other low Mo alloys provided other relevant parameters are evaluated and found favourable.

References

[1] G.L. Hofman, L.C. Walters, Metallic fast reactor fuels, Mater. Sci. Tech, 1994, 10A, 3.

[2] S. Das, et al., Characterisation of microstructural, mechanical and thermophysical properties of Th-52U alloy, J. Nucl. Mater., 2016, 480, 223–234.

[3] S.Das, et al., Characterisation of microstructural, mechanical and thermal properties and ageing study of the Th-3wt%U alloy, Nucl. Eng. Des. 282 (2015) 116–125.

[4] N. Clavier, R. Podor, L. Deliere, J. Ravaux, N. Dacheux. Combining in situ HT-ESEM observations and dilatometry: an original and fast way to the sintering map of ThO_2. Mater. Chem. Phys., 2013, 137, 3, 742–749.

[5] N. Hingant, N. Clavier, N., Dacheux, S. Hubert, N. Barre, R. Podor, L. Aranda, Preparation of morphology controlled $Th_{1-x}U_xO_2$ sintered pellets from low temperature precursors, Powder

Table 7 : Phase fraction and lattice parameter data for Th-30U-1Mo (X-ray diffraction) obtained by Rietveld method.

Phase	Space group	Phase fraction (%)	a (Å)	b (Å)	c (Å)	Angles
Th	F m - 3 m	77.48 ± 2.23	5.073(6)	5.073(6)	5.073(6)	α = 90°; ß = 90°; γ = 90°
α- U	C m c m	8.59 ± 0.66	2.855(9)	5.952(5)	4.962(3)	α = 90°; ß = 90°; γ = 90°
ThO_2	F m - 3 m	13.93 ± 1.17	5.582(5)	5.582(5)	5.582(5)	α = 90°; ß = 90°; γ = 90°

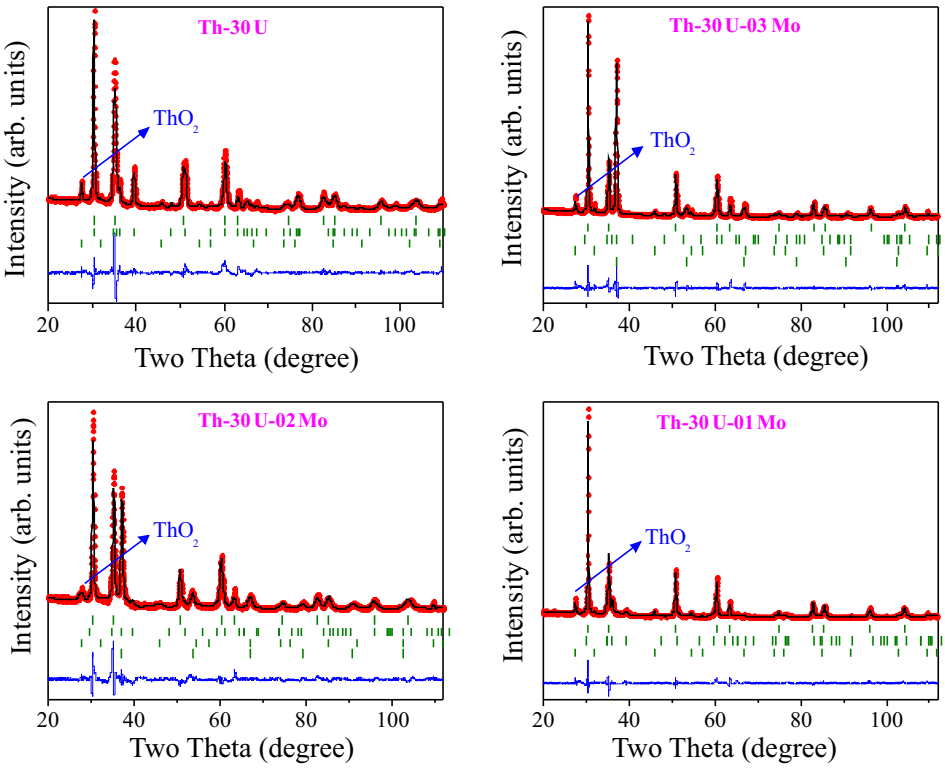

Fig.5: Rietveld refinement fit of Th-30U-Mo alloy samples : X-ray Diffraction.

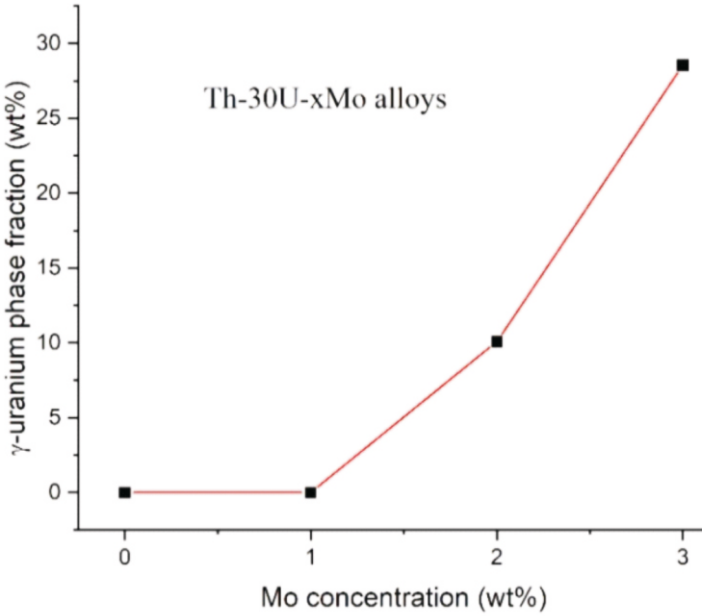

Fig.6: γ-U phase fraction in Th-30U-Mo alloy samples with respect to Mo concentration.

Technol., 2011, 208, 2, 454–460.

[6] W.J. Carmack, D.L. Porter, Y.I. Chang, S.L. Hayes, M.K. Meyer, D.E. Burkes, C.B. Lee, T. Mizuno, F. Delage, J. Somers,Metallic fuels for advanced reactors. J.Nucl. Mater., 2009, 392, 2, 139–150.

[7] S. Kaity, J. Banerjee, M.R. Nair, K. Ravi, S. Dash, T.R.G. Kutty, A. Kumar R.P. Singh. Microstructural and thermophysical properties of U–6wt%Zr alloyfor fast reactor application. J. Nucl. Mater., 2012, 427, 1–11.

[8] O. Benes, D.Manara, R.J.M. Kornings. Thermodynamic assessment of the Th–U–Pu system. J. Nucl. Mater., 2014, 449, 15–22.

[9] IAEA, Status and Trends of Nuclear Fuels for Sodium Cooled Fast Reactors, IAEA, Vienna, 2011.

[10] J.H. Kittel, J.A.Horak, W.F. Murphy, S.H. Paine, Effects of Irradiation on Tho-rium and Thorium–Uranium Alloys, USAEC, ANL-4574, 1963.

[11] S. Das, S. Kaity, R. Kumar, J. Banerjee, S.B. Roy, G.P. Chaudhari, B.S.S. Daniel, Determination of Room Temperature Thermal Conductivity of Thorium—Uranium Alloys. In Thorium—Energy for the Future. Springer, Singapore, 2019, 277-286.

[12] S. Das, S.B. Roy, G.P. Chaudhari, B.S.S. Daniel, Microstructural evolution of as-cast Th-U alloys, Prog. Nucl. Energy, 2016, 88, 285-296.

[13] Thorium Fuel Cycle-Potential Benefits and Challenges, IAEA, Vienna, 2005. IAEA-TECDOC-1450 ISSN1011-4289.

[14] R. Kumar, S. Das, S.B. Roy, R. Agarwal, J. Banerjee, & S.K. Satpati, Effect of Mo addition on the microstructural evolution and γ-U stability in Th-U alloys. Journal of Nuclear Materials, 2020, 539, 152317.

[15] P. Rodriguez and C. V. Sundaram, Nuclear and Material Aspects of The Thorium Fuel Cycle, Journal of Nuclear Materials, 1981, 100 227-249.

[16] G.L. Copeland, Evaluation of thorium-uranium alloys for the unclad metal breeder reactor, ORNL, Oak Ridge, ORNL-4557, 1970.

[17] M.S. Farkas, A.A. Bauer, R.F. Dickerson, Development of Th-U Base Fuel Alloys, BMI, Ohio, 1960, BMI-1428.

[18] A.E. Walter, D.R. Todd, P.V. Tsvetkov, Fast Spectrum Reactors,14419957 14th ed., Springer Science Business Media LLC, USA, 2012.

[19] J.H. Kittel, J.A. Horak, W.F. Murphy, J.H. Paine, Effects of Irradiation on Thorium and Thorium Alloys, ANL, Illnios, 1963, ANL-5674.

[20] R. Prabhakaran, D.E. Burkes, D.M. Wachs, J.I. Cole, I.Charit, Small Scale Specimen Testing of Monolithic U-Mo Fuel Foils, Idaho National Laboratory, Washington, D.C, RERTR, 2008, Meeting INL/CON-08-14612.

[21] A. Landa, P. Soderlind, P.E.A. Turchi, Density Functional Study of U-Mo and UZr Alloys, Lawrence Livermore National Laboratory, US, 2010, LLNL-JRNL-461538.

[22] S. Jana, et al., Kinetics of cellular transformation and competing precipitation mechanisms during sub-eutectoid annealing of U10Mo alloys, J. Alloys Compd., 2017, 723, 757-771.

[23] G.G. Bentle, Study of the Thorium-Uranium alloy system, in: IAEA Conference Paper, Geneva, 1958, pp. 706.

[24] G.H. Bannister, J.R. Thomson, The bcc to fcc phase transformation in thoriumand some thorium rich alloys, J. Nucl. Mater., 1964, 12, 1, 16-23.

[25] B.R. Hayward, P. Corzine, Thorium-uranium fuel elements for SRE, in: 2nd International Conference on the Peaceful Uses of Atomic Energy, Geneva, 1958, pp. 785.

[26] M.A. Steiner, E. Garlea, S.R. Agnew, Modeling solute segregation during the solidification of γ-phase U-Mo alloys, J. Nucl. Mater., 2016, 474, 105-112.

[27] O.D. McMasters, P.E. Palmer, W.L. Larsen, Th-Mo Phase diagram, J. Nucl. Mater., 1964, 7, 3, 151-156.

[28] S.Neogy, et al., Microstructural study of gamma phase stability in U-9wt%Mo alloy, J. Nucl. Mater., 2012, 422, 77-85.

[29] J.P. Hammond, Review of information on U-Mo alloys and U-Mo-UO_2 dispersion fuels, ORNL, ORNL60- 6-L22, 1960.

[30] N.-T.H. Kim-Ngan, I. Tkatch, S. Maskova, A.P. Goncalves, L. Havela, Study of decomposition and stabilisation of splat-cooled cubic gamma phase U-Mo alloys, J. Alloys Compd., 2013, 580, 223-231.